Proceedings of ICONE14
International Conference on Nuclear Engineering
July 17-20, Miami, Florida, USA

ICONE14-89120

BUOYANCY DRIVEN COOLANT MIXING STUDIES OF NATURAL CIRCULATION FLOWS AT THE ROCOM TEST FACILITY USING ANSYS CFX

Thomas Höhne, Sören Kliem, Ulrich Rohde, Frank-Peter Weiß

Forschungszentrum Rossendorf - Institute of Safety Research
P.Box 510119, D-01314 Dresden, Germany
Phone: (+49) 351 260 2425
e-mail: T.Hoehne@fz-rossendorf.de

ABSTRACT

Coolant mixing in the cold leg, downcomer and the lower plenum of pressurized water reactors is an important phenomenon mitigating the reactivity insertion into the core. Therefore, mixing of the de-borated slugs with the ambient coolant in the reactor pressure vessel was investigated at the four loop 1:5 scaled ROCOM mixing test facility. Thermal hydraulics analyses showed, that weakly borated condensate can accumulate in particular in the pump loop seal of those loops, which do not receive safety injection. After refilling of the primary circuit, natural circulation in the stagnant loops can re-establish simultaneously and the de-borated slugs are shifted towards the reactor pressure vessel (RPV).

In the ROCOM experiments, the length of the flow ramp and the initial density difference between the slugs and the ambient coolant was varied. From the test matrix experiments with 0 resp. 2% density difference between the de-borated slugs and the ambient coolant were used to validate the CFD software *ANSYS CFX*. To model the effects of turbulence on the mean flow a higher order Reynolds stress turbulence model was employed and a mesh consisting of 6.4 million hybrid elements was utilized. Only the experiments and CFD calculations with modeled density differences show a stratification in the downcomer. Depending on the degree of density differences the less dense slugs flow around the core barrel at the top of the downcomer. At the opposite side the lower borated coolant is entrained by the colder safety injection water and transported to the core. The validation proves that *ANSYS CFX* is able to simulate appropriately the flow field and mixing effects of coolant with different densities.

INTRODUCTION

A small break loss of coolant accident (SBLOCA) can lead to the interruption of one-phase flow natural circulation in the loops of a pressurized water reactor (PWR). This could happen when the high pressure safety injection (HPSI) should be partly unavailable. In such cases, a part of the decay heat is removed from the core in the reflux-condenser mode. This leads to the production and accumulation of low borated coolant in the primary circuit. The primary system will be filled up again and one-phase natural circulation re-establishes. The one phase natural circulation forwards the under-borated condensate towards the core.

By theoretical analyses using the thermal-hydraulic system code *ATHLET*, the Gesellschaft für Reaktorsicherheit (GRS) revealed a special scenario which could possibly occur after a SBLOCA in the hot leg and safety injection into two hot legs (Pointner, 2003). According to these *ATHLET*-calculations this scenario can happen at higher decay heat power levels, only. Then the steam mass flow rate produced in the core reaches 200 kg/s or is even higher. Due to counter current flow limitation of the safety injection against the steam up-flowing from the core, the safety injection cannot enter the upper plenum but flows to the steam generators (SG). In this way one-phase natural circulation is maintained in those two loops obtaining safety injection. The other two loops will operate in reflux-condenser mode and all the condensate will accumulate there. Since the temperature of the coolant entering the SGs that run in one-phase flow is lower than the secondary side temperature, the safety injection water is even heated by the secondary side. This secondary to primary heating power still adds to the decay heat level. The situation with two loops remaining in one-phase flow and the other two simultaneously turning back to one-phase flow after refilling the RPV is

suspected extremely disadvantageous in terms of mixing of the condensate with the ambient coolant in the downcomer (DC) and the lower plenum (LP). For that reason the slug might reach the core with low boron concentration.

For a better understanding of the basic phenomena of boron dilution in pressurized water reactors (PWR) experimental investigations were performed in three test facilities. These are the Primärkreislauf (PKL) facility and the Upper Plenum Test Facility (UPTF), both operated by Framatome ANP, and the Rossendorf Coolant Mixing Model (ROCOM), operated by the Forschungszentrum Rossendorf e.V. A detailed description of the ROCOM experiments is shown in (Kliem et al., 2004)

For *ANSYS CFX* validation two ROCOM test cases, one with density driven coolant mixing (e.g. start of natural convection in two loops at the same time with a steep ramp, slugs with 2% lower density coolant are representing a reactor volume of 7.2 m³) and for comparison one without density differences but using the same flow conditions were selected from the test matrix (see Table 1). The experiments and the CFD-calculations described in this paper were performed to investigate the coolant mixing in the RPV. Similar analyses using the CFD-Code *FLUENT* were performed by Schaffrath et al. (2005).

ROSSENDORF COOLANT MIXING MODEL (ROCOM)

The Rossendorf Coolant Mixing Model (ROCOM) was constructed at the Forschungszentrum Rossendorf e.V. (FZR) for the investigation of coolant mixing in PWR (Grunwald et al., 2002 and Höhne et al., 2003). The ROCOM facility has four loops each with an individually controlled pump (see Fig. 1). This allows to perform tests in a wide range of PWR flow conditions from natural convection flow up to forced convection flow at nominal flow rates including flow ramps (e.g. due to pump start up). ROCOM is operated with water at ambient temperatures because the reactor pressure vessel (RPV) mock-up and its internals are made of perspex. Special attention to all

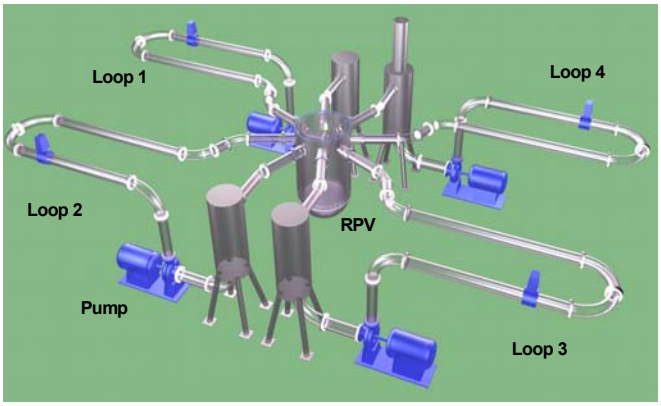

Fig. 1 Scheme of ROCOM

components that significantly influence the velocity fields. These are the core barrel with the lower support plate and the core simulator, the perforated drum in the lower plenum and the inlet and outlet nozzles of the main coolant lines with diffuser elements.

The model has a the linear scale is 1:5 to the prototype, the water inventory in the loops is kept in scale 1:125 and the traveling time of the coolant is identical to the original reactor.

To ensure the transferability of the measured concentration fields to the reactor the Strouhal (Sr) and Froude number (Fr), which are defined as

$$Sr = \frac{l}{v\,\tau} \tag{1}$$

and

$$Fr = \sqrt{\frac{\rho v^2}{\Delta\rho\, g\, l}} \tag{2}$$

must be adhered. In the definitions above l denotes the characteristic length, v the velocity, τ the characteristic time, ρ the coolant density, Δρ the density difference between the borated and the unborated coolant, and g the acceleration of gravity. The Froude number is a criteria to distinguish between momentum controlled and buoyancy driven flows. In cases of high turbulent velocity fields and negligible coolant density differences there is almost no influence of the Reynolds number

$$\mathrm{Re} = \frac{l\,v}{\nu}\ , \tag{3}$$

on the velocity field and the experimental data can be transferred directly to the reactor because of the scale down of length and velocity (Dräger, 1987 and Hertlein et al., 2003). In the definition of the Reynolds number ν denotes the kinematic viscosity.

During inherent dilution the slug could have a higher temperature and a lower density. Additionally the boron content influences the fluid density. In ROCOM this density difference is adjusted by the addition of ethyl alcohol.

The acquisition of the concentration fields is performed with high spatial and temporal resolution measurements of the tracer concentration. For that purpose FZR introduces self developed wire mesh sensors which measure the electrical conductivity between two orthogonal electrode grids (Prasser et al., 1998). Beside the measurements in the cold legs, two further wire-mesh sensors with 4 radial and 64 azimuthal measuring positions in the downcomer and 193 conductivity measurements at the core entrance were applied to the test facility. All sensors provide 200 measurements per second. Because a measuring frequency of 20 Hz is sufficient, ten successive images are averaged into one conductivity distribution.

The measured conductivity values are transformed into a dimensionless mixing scalar $\Theta_{x,y,z}(t)$. It is calculated by relating the local instantaneous conductivity $\sigma_{x,y,z}(t)$ to the amplitude of the conductivity change in the cold leg of the loops with the slugs.

$$\Theta_{x,y,z}(t) = \frac{\sigma_{x,y,z}(t) - \sigma_0}{\sigma_1 - \sigma_0} \qquad (4)$$

Θ represents the contribution of the coolant from the initial slugs to the mixture at the given position x,y,z. The upper reference value σ_1 in (4) is the conductivity in the initial slugs between the gate valves. The lower reference value σ_0 is the initial conductivity of the water in the test facility before the valves are opened.

More details about the facility, the measurement devices, and the experiments performed earlier can be found in (Grunwald et al., 2003).

Based on *ATHLET*-calculations in (Pointner, 2003), the following boundary conditions were defined for the experiments: Two loops are working at a stationary level of 5 % of the nominal flow rate. A slug of de-borated water is located in both of the resting loops. The volume of these de-borated slugs corresponds to the volume of the whole loop seal and a part of the steam generator outlet chamber. This is 7.2 m^3 in each loop. In these loops, the circulation starts simultaneously and reaches a value of 6 % of the nominal flow rate. Three different lengths of the flow ramp were considered.

Further, according to the thermo-hydraulic calculations, a density difference exists between the de-borated slugs and the ambient coolant. This is due to the higher temperature of the slug in comparison to the ambient coolant. The concentration difference between borated and de-borated coolant creates an additional density difference. To investigate the influence of the density difference, it was decided to vary this difference between 0 and 2 %.

On that basis the following experimental matrix was created:

Table 1 Matrix of the experiments

	Density difference [%]	0	0.25	0.5	1.0	2.0
N°	ramp length [s]					
1	25 (18)	5* TEST I	1	1	5	5* TEST II
2	50 (40)	5	-	-	-	5
3	75 (61)	5	-	-	-	5

*The boundary conditions of these experiments were used for code validation.

The length of the flow ramp given in Tab. 1 is the duration of the frequency ramp of the pump control system. Due to the inertia of the pumps and the coolant, the circulation starts with a delay. Therefore, the measured flow ramps are shorter than the frequency ramps. The duration of the flow ramps is indicated in parentheses. The numbers in the table says how many times the experiment was repeated. The repetition was made to damp statistical fluctuations. The presented results were obtained by averaging over the indicated number of single realizations. An error analysis for the ROCOM test facility measurements was done in (Kliem, 2003). The conclusions on the error assessment are:

- The discretisation error and the error caused by statistical fluctuations of the signal are one magnitude smaller than the calibration error.
- An higher amplitude of the perturbation (use of the maximal possible increase of the conductivity) in the experiments decreases the absolute error of the mixing scalar.
- The error of the mixing scalar does not depend on the primary measurement value itself.
- The calculated error bands for the measurement positions of one sensor show small differences, only.
- The calculated error bands are clearly smaller than the fluctuations of the measured values caused by the turbulent nature of the flow in the test facility.
- The biggest error of the mixing coefficient found at the core inlet was in the range of 4 %.

CFD CODE AND SENSITIVITY ANALYSIS ACCORDING TO BEST PRACTICE GUIDELINES

The CFD code for simulating the mixing studies was *ANSYS CFX* (ANSYS CFX, 2005). *ANSYS CFX* is an element-based finite-volume method with second-order discretisation schemes in space and time. It uses a coupled algebraic multigrid algorithm to solve the linear systems arising from discretisation. The discretisation schemes and the multigrid solver are scalably parallelized. *ANSYS CFX* works with unstructured hybrid grids consisting of tet, hex, prism and pyramid elements.

Numerical diffusion, nodalization, time step size and turbulence modelling

The overall error of a CFD calculation is a combination of several aspects: Grid density, discretisation method, time step size, iteration error and the employed mathematical models all have their own effect. The separation of these error components for complex three-dimensional calculation is difficult. For example discretisation errors can act like an additional numerical diffusivity, and can affect the results in a similar way as a too large eddy viscosity arising from an unsuitable turbulence model.

Discretisation errors can be reduced by using finer grids, higher-order discretisation methods and smaller time step sizes. However, in many practical three-dimensional applications grid- and time step-independent solutions cannot be obtained because of hardware limitations. In these cases, the remaining errors and uncertainties should be quantified as described in the

Best Practice Guidelines (BPG) by Menter et al. (2002). In the current study, the CFD simulations were performed according to these BPGs. A convergence criterion of 1×10^{-4} was used to ensure negligibly small iteration errors (Domain Imbalances: U-Mom -0.0051 %, V-Mom 0.0073 %, W-Mom -0.0007 %, P-Mass -0.0001 %, AL-Mass faction 0.0433 %).

In the recent calculations shown below, the High-Resolution (HR) discretisation scheme of *ANSYS CFX* was used to discretize the convective terms in the model equations. A second-order implicit scheme was used to approximate the transient terms. The used time step size used was 0.1 s. The ethyl alcohol water, which had a lower density, was used as a tracer. It was modeled with the multi-component model of *ANSYS CFX*. In a multi-component flow, the components share the same velocity, pressure and temperature fields. The properties of multi-component fluids are calculated on the assumption that the constituent components form an ideal mixture. The ethyl alcohol water is modeled as a component with different density and viscosity compared to water. The mass fraction of the ethyl alcohol water can be directly related to the mixing scalar described in Eq. (4). The Reynolds stress model proposed by Launder et al. (1975) was used in combination with an ω-based length scale equation (BSL model) to model the effects of turbulence on the mean flow. Buoyancy production terms were included in the Reynolds stress equations and in the length-scale equation. The buoyancy production terms in the Reynolds stress equations are exact terms and require no modeling. A transient of 150 s was simulated.

The calculations on 8 processors of a 100-processor RedHat LINUX cluster (dual CPU compute nodes XEON, 3.2 GHz, ~1.3 Gflops, each containing 2 GBytes RAM) took 2 weeks.

Geometrical Details

The geometric details of the ROCOM internals have a strong influence on the flow field and on the mixing. Therefore, an exact representation of the inlet region, the downcomer below the inlet region, and the obstruction of the flow by the outlet nozzles in the downcomer is necessary. In the current study, these geometric details were modeled using the *ICEM CFD* software.

The final model included all relevant parts of the four loops, the inlet nozzles with the diffuser part, the orifices of the outlet nozzles, the downcomer extension, the lower plenum, the core support plate, the perforated drum, the core simulator, the upper plenum, and the outlet nozzles (Fig. 3 and 4). The perforated drum, shown in Fig 2, contains 410 orifices of 15 mm diameter. In addition to previous work with the block structured code *CFX-4* (Höhne, 2003) the drum could be modeled in detail utilizing the multigrid solver of *ANSYS CFX*. The advantage is a detailed study of the flow phenomena in the lower plenum, the disadvantage is the high numerical effort.

Sensitivity tests analyzing the influence of different ways of modeling the perforated drum (e.g. porous media, resistant coefficients, reduced number of holes) are presented in (Hemström, 2005). The core contains 193 fuel element dummies. Although it was found in (Hemström, 2005), that the influence of the core structure and upper plenum on the flow and mixing pattern at the core inlet is rather small, also these regions were modeled in detail (Fig. 4).

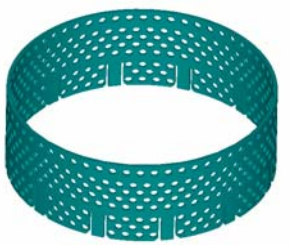

Fig. 2 Perforated drum (*ANSYS CFX*)

Grid Generation

The mesh was generated with the *ICEM CFD* software. It consisted of 3.6 million nodes and 6.5 million hybrid elements (Fig 3, Table 2). The mesh was refined at the perforated drum, in the lower support plate and at the wall regions of the cold legs. The downcomer and nozzle region was discretized with hexahedral cells; tetrahedral elements were used for the lower plenum (Fig.4).

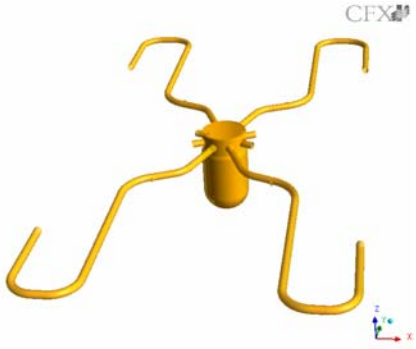

Fig. 3 Flow domain with inlet boundary conditions

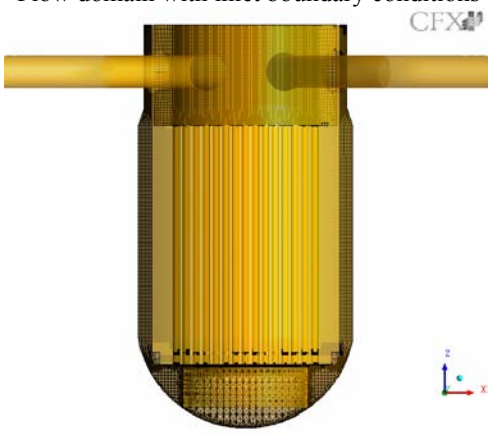

Fig. 4 Hybrid Mesh vertical cut

Table 2 Grid information

Grid Type	Size	Mesh generator	Code
HYBRID	Nodes: 3643122 Elements: 6488817 Tetrahedrals, Wedges, Pyramids, Hexahedrals	*ICEM CFD*	*ANSYS CFX*

Boundary Conditions

For *ANSYS CFX* validation two tests, one without density differences (TEST I) and one test with density driven coolant mixing (TEST II) were selected from the test matrix, which is characterized by flow rates which are typical for natural convection conditions and a steep flow ramp after pump start up in the test run.

These tests were performed under the following initial and boundary conditions which were also adjusted in the *ANSYS CFX* calculation (Fig. 5):

- the loops 3 and 4 are operated with 5% of the nominal flow rate (9.25 m³/h),
- TEST I: slugs of water with no density differences to the coolant inventory are introduced in the bends between the valves in loop 1 and 2,
- TEST II: slugs of water with 2% lower density are introduced in the bends (the density decrease is achieved by mixing water with alcohol),
- the flow rate in loop 1 and 2 is increased from 0 to 6% of the nominal flow in 18 s.

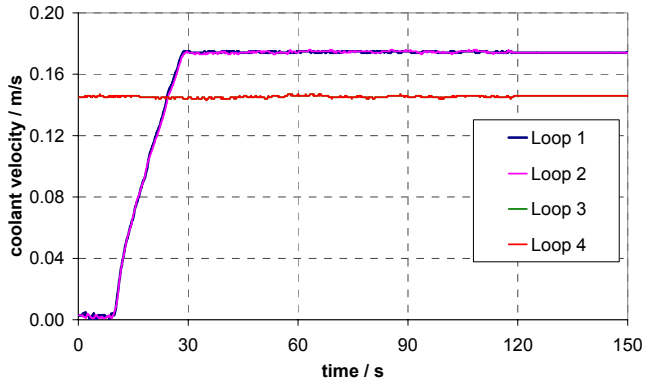

Fig. 5 Coolant velocities in the four loops during the experiment

COMPUTATIONAL RESULTS OF TEST I AND II

Qualitative Analysis

In Fig. 6 the alcohol mass fraction of the coolant (water with lower density) in loop 1 and 2, hereafter called mixing scalar, of TEST II is shown at 40 s after start of the simulation. The slugs with the lower density are transported through the cold legs towards the downcomer. On the way to the RPV mock-up inlet the flow stratifies. The lower density coolant flows in the upper part of the pipe cross section area and the higher density coolant in its lower part. After 40 s the slug with the lower density has reached the inlet nozzles of the RPV mock-up and the downcomer.

Fig. 7 shows the mixing scalar distribution in the unwrapped downcomer of TEST II at 50, 55 and 62 s. After 50s the slug has reached the upper measuring level of the downcomer. Already at this level nearly the whole cross section of the downcomer is filled with lower density coolant. After 60 s the lower density coolant reaches the lower measuring level of the downcomer. The lower density coolant is detected at the opposite side of the inlet nozzles of loop 1 and 2 first. This phenomenon can be explained as follows: the low density coolant rises after introduction into the RPV mock-up above the inlet nozzle level. Then it flows in circumferential direction to the inlet nozzles of the loops 3 and 4. Here the lower density coolant mixes with the higher density coolant of the loops 3 and 4 and flows downwards. At the lower measurement level of the downcomer the maximum of the mixing scalar has decreased approx. by a factor of 2.5.

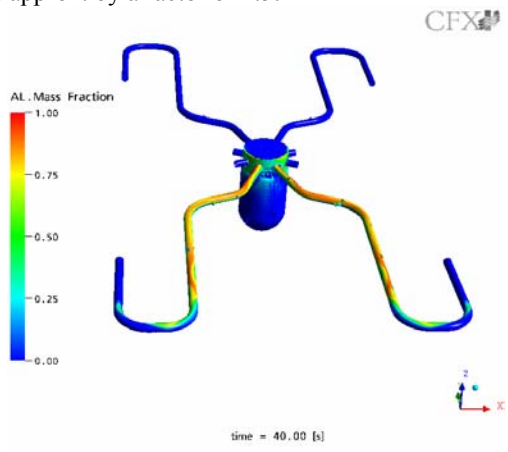

AL.Mass Fraction (Mixing Scalar)

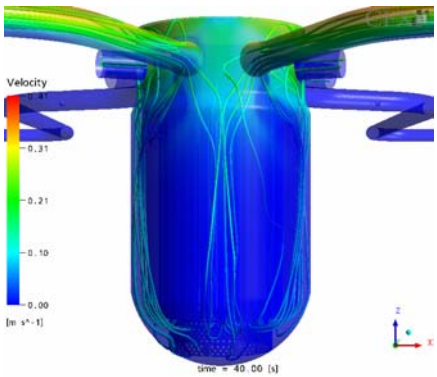

Flow field (Streamlines)

Fig. 6 Instantaneous mixing scalar distributions and streamlines representing the velocity field at 40s; TESTII

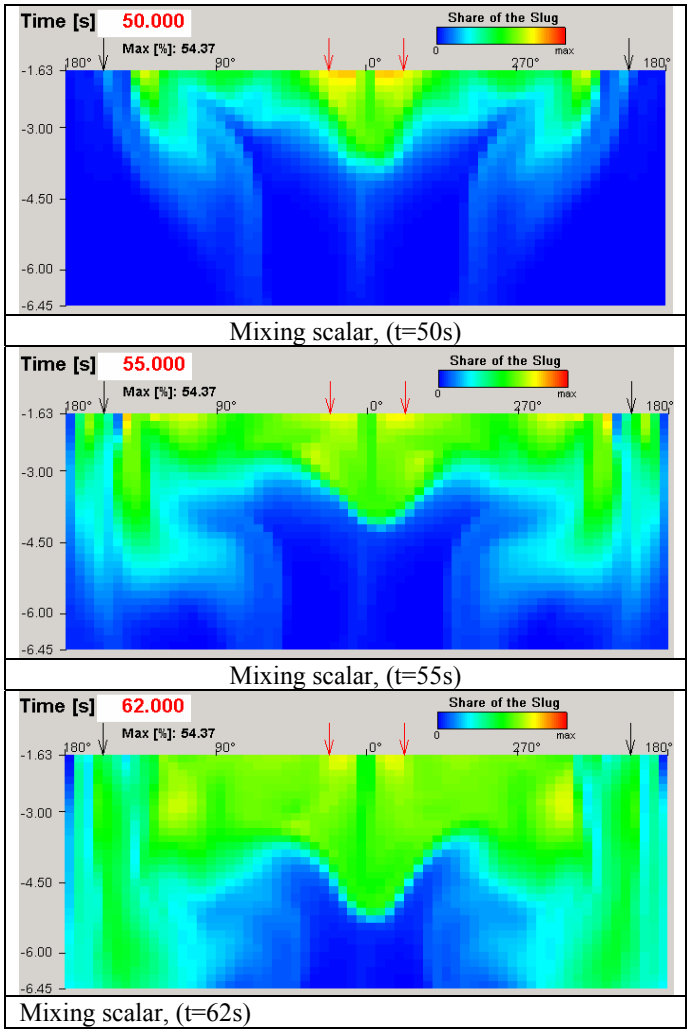

Fig. 7 Mixing scalar distribution in the unwrapped downcomer, TEST II

Figures 8 resp. 9 illustrate the mixing scalar distribution in the unwrapped upper and lower downcomer sensor for the experiment and the CFD calculation for the TEST I resp. II. At the top of the Figures, the maximum values for the mixing scalar are added and the red arrow indicates the position of the loops with the running pumps. Fig. 8 (TEST I, no density differences) shows, that the mixing scalar is mainly distributed below the indicated loops with three maxima at the upper and lower downcomer sensor and therefore show a sector formation. In contrast in Fig. 9 (TEST II, 2% density differences) the upper downcomer is filled up with the lighter tracered water and due to the transportation of the running loops 3 and 4 the mixing scalar first arrives in the lower downcomer at the opposite side of loop 1 and 2. The maximum values of the mixing scalar indicate, that there is almost no mixing in the downcomer region in TEST I (experiment upper downcomer 90%, lower downcomer 86%), while in TEST II the maximum value reduces from 91% to 40% due to enhanced mixing caused by the density differences of the coolant inventory.

The shape of the mixing scalar distribution is almost identical between the experiments and the numerical results, although the turbulent structure at the lower downcomer position is less intense at the calculation, probably due to the limitations of the used RSM turbulence model.

The qualitative pictures of the *ANSYS CFX* simulation show, that this CFD code is able to simulate appropriately the transport and mixing phenomena e.g. such effects like streaks of coolant with lower density in the downcomer and stratification of the fluid flow in the reactor coolant line.

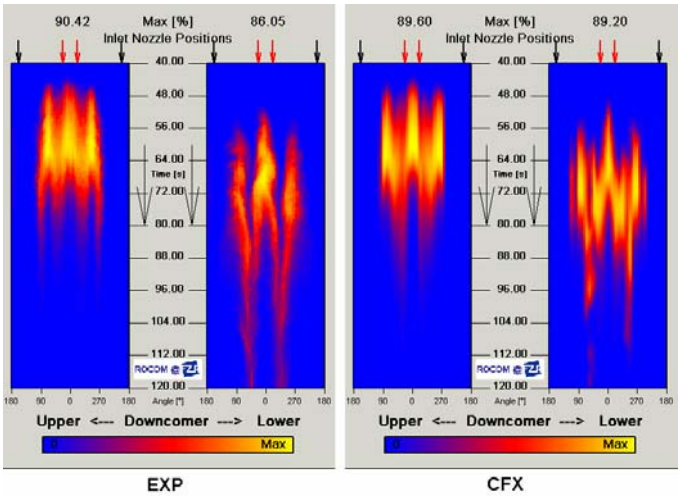

Fig. 8 Instantaneous azimuthal mixing scalar distributions for the 32 positions of the upper and lower downcomer sensor, TEST I

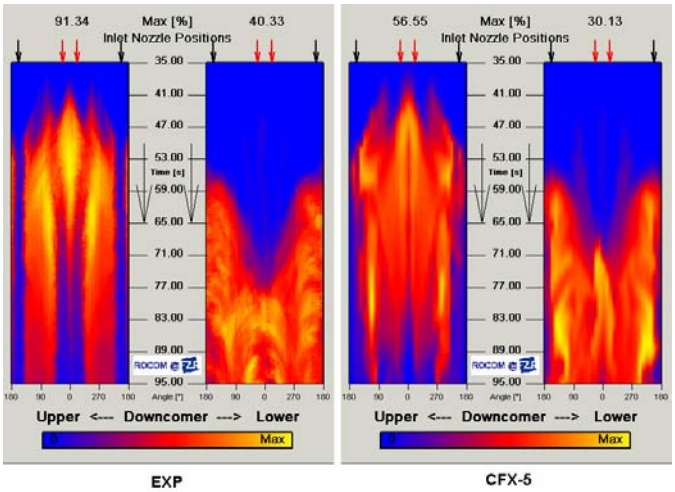

Fig. 9 Instantaneous azimuthal mixing scalar distributions for the 32 positions of the upper and lower downcomer sensor, TEST II

Quantitative Analysis

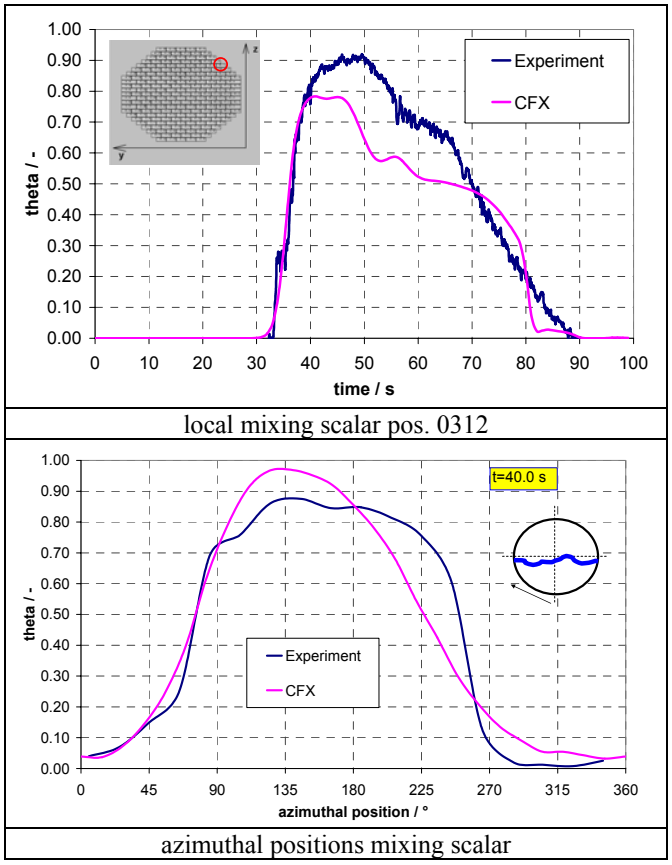

Fig. 10 Time dependent mixing scalar distributions at the cold leg, inlet nozzle sensor, TEST II

Turbulent, natural convection flows are characterized by hydraulically instable conditions and small driving forces what obviously yield in non-stationary flow fields. A quantitative comparison of experiments and calculations is therefore difficult. The general agreement of the courses of the dominant quantities is thus the only way to asses a calculation. Local discrepancies in the transient courses are inevitably present in such comparisons due to statistical turbulent mixing effects.

In general, the code *ANSYS CFX* represent correctly the instantaneous azimuthal distribution of the mixing scalar in the downcomer. Discrepancies can not only be addressed to code and modeling differences but also to the instationary and indeterministic character of turbulent flow.

Fig. 10 shows one local measurement point (position 0312 at the upper part) and the circumferential distribution of the mixing scalar at the outer wall of the cold leg sensor for TEST II at 40s. The 0°-position is at the bottom of the cold leg. The calculations reflect the observed stratification of lighter water (tracer) on top of the heavier water of the experiment. The arriving time of the slug is well predicted. The calculation shows already in the cold leg a more intense mixing behavior than it is observed in the experiment (smaller maximum values of the mixing scalar at 50s).

Thirty two circumferential sensor positions in the middle of the upper and lower downcomer sensor plane were selected for comparison of data and predictions (Figures 11 and 12). For a better understanding, the azimuthal direction of the sensor positions as well as their locations along a line are added to the top of the Fig. 11. The arrangement of the cold leg nozzles 1 and 4 is also added to this Figure.

Fig. 12 shows the instantaneous azimuthal mixing scalar distributions of the upper (at 50s) and lower downcomer (at 90s) sensor for TEST I.

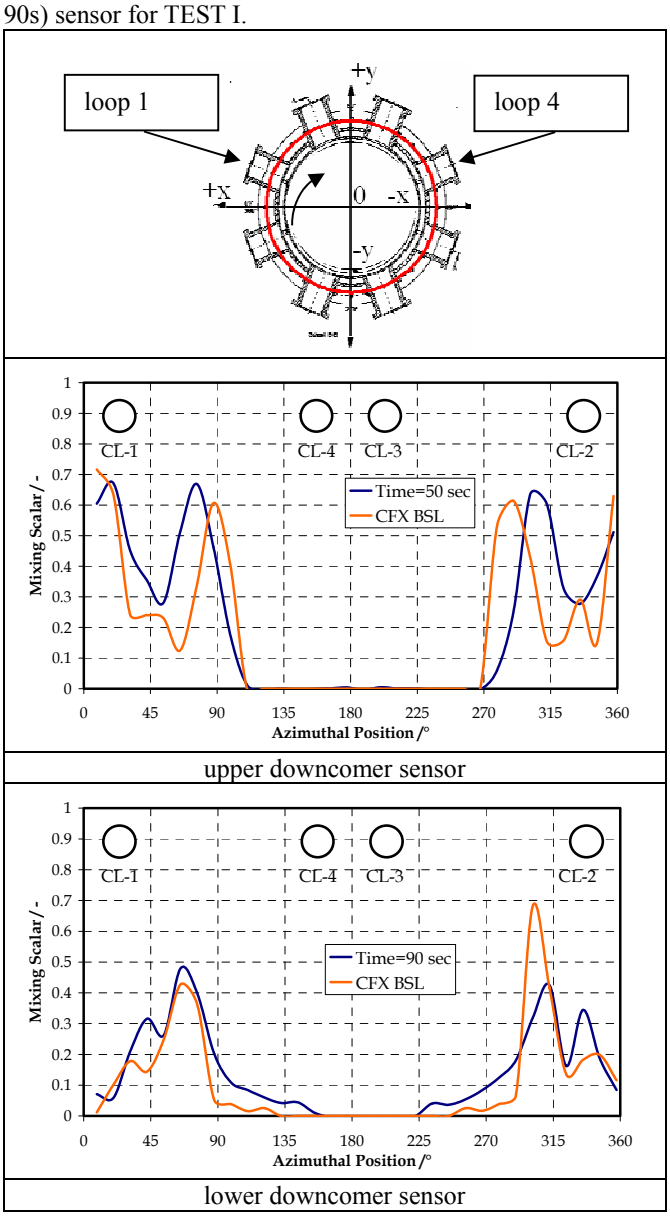

Fig. 11 Instantaneous azimuthal mixing scalar distributions for positions of the upper (at 50s) and lower downcomer (at 90s) sensor, TEST I

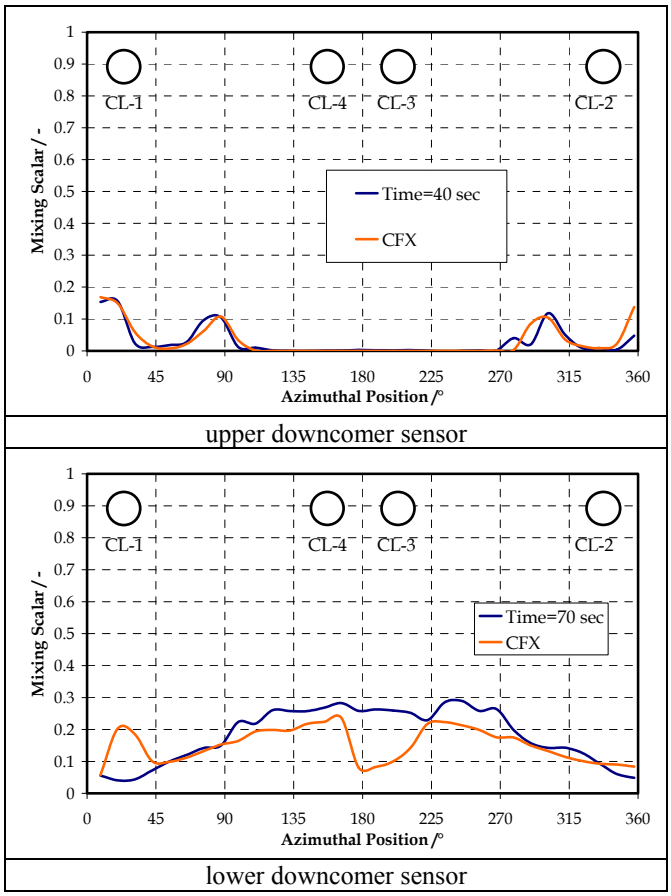

Fig. 12 Instantaneous azimuthal mixing scalar distributions for positions of the upper (at 40s) and lower (at 70s) downcomer sensor, TEST II

The Figure 11 shows the azimuthal maxima of the mixing scalar at 50s in the upper downcomer below the inlet nozzles of the loops 1 and 2. The positions of these maxima remain also at the lower downcomer at 90s.

The circumferential distributions of the mixing scalar of TEST II at the downcomer sensors at 40s resp. 70s in Fig. 12 show the arrival of the slug in the upper downcomer below the inlet nozzles of loop 1 and 2 and the maximum of the mixing scalar at the lower downcomer with generally lower values at the opposite side of loop 1 and 2 (below the loops 3 and 4).

The shape of the perturbations of experiment and CFD simulation is almost identical in both cases (TEST I and II).

CONCLUSIONS AND OUTLOOK

Mixing after injection of de-borated slugs into the RPV was investigated under simulated natural circulation conditions at the four loop 1:5 scaled test facility ROCOM. The corresponding boundary conditions were derived from calculations with the system code *ATHLET* for a postulated hypothetical SB LOCA scenario. In the experiments, the length of the flow ramp and the initial density difference between the slugs and the ambient coolant was varied.

Experiments with 0% (TEST I) resp. 2% (TEST II) density difference between the de-borated slugs and the ambient coolant were used to validate the CFD software *ANSYS CFX*. A Reynolds stress turbulence model was employed to model the effects of turbulence on the mean flow. A hybrid mesh consisting of 3.6 million nodes and 6.4 million elements was utilized.

The experiment and CFD calculation of TEST I show a sector formation below loop 1 and 2, while in TEST II the de-borated slugs stratify in the cold leg and in the downcomer. The less dense slugs flow around the core barrel at the top of the downcomer. On the opposite side the lower borated coolant is entrained by the colder safety injection water and transported to the core.

The *ANSYS CFX* calculations show a good qualitative agreement with the experimental data. At some local positions differences in the predicted and measured concentration fields occur.

The obtained experimental and numerical results can be used for further studies of the core behavior using coupled thermo-hydraulic and neutron-kinetic code systems.

ACKNOWLEDGMENTS

The project this paper is based on was funded by the Nuclear Special Committee “Plant engineering” of VGB PowerTech (Germany).

REFERENCES

ANSYS CFX User Manual. *ANSYS-CFX*. 2005.

Dräger, P. Macroscopic coolant mixing in pressurized water reactors. *PhD, TH Zittau*, Germany. 1987.

F. Menter. CFD Best Practice Guidelines for CFD Code Validation for Reactor Safety Applications. *ECORA FIKS-CT-2001-00154*. 2002.

S. Kliem, U. Rohde, B. Hemström, T. Toppila, Y. Bezrukov, Description of the slug mixing and buoyancy related experiments at the different test facilities, *Deliverable D09, FIKS-CT-2001-00197*, 2003

Grunwald, G., Höhne, T., Kliem, S., Prasser, H.-M., Rohde, U. Experimentelle Untersuchung der Kühlmittelvermischung unter den Bedingungen wiederanlaufenden Naturumlaufes. Final Report, *VGB SA “AT” 29/01*. 2003 (confidential).

Grunwald, G., Höhne, T., Kliem, S., Prasser, Richter, K.-H., H.-M., Rohde, U., Weiss, F.-P. Versuchsanlage ROCOM zur Untersuchung der Kühlmittelvermischung in Druckwasserreaktoren - Ergebnisse quasistationärer Vermischungsexperimente. *FZR Report 348*. 2002.

Hemström, B., et al. Validation of CFD codes based on mixing experiments (Final report on WP4). *EU/FP5 FLOMIX-R report, FLOMIX-R-D11*. Vattenfall Utveckling (Sweden). 2005.

Hertlein, R., Umminger, K., Kliem, S., Prasser, H.-M., Höhne, T. and Weiss, F.-P. Experimental and numerical investigation of boron dilution transients in pressurized water reactors. *Nuclear Technology 141,* 88 - 106. 2003.

Höhne, T., Kliem, Prasser, H.-M., Rohde, U. Experimental and numerical studies inside a reactor pressure vessel. *4th ASME/JSME Joint Fluids Engineering Conference*, Hawaii, USA. CD-ROM. 2003.

Kliem S., Höhne, T., Prasser, H.-M., Rohde, U. Weiss, F.-P. Experimental investigation of coolant mixing in the RPV of a PWR during natural circulation conditions. Proceedings of *ICONE12, 12th International Conference on Nuclear Engineering*, Washington D.C., USA, April 25-29 2004. paper 49424. 2004.

Launder, B.E. - Reece, G.J. - Rodi, W. Progress in the Development of a Reynolds-Stress Turbulence Closure. *J. Fluid Mech.* 68(3):537-566. 1975.

Pointner, W. and Wohlstein, R. Initiating events and scenarios of boron dilution transients (in German). *Annual meeting on Nuclear Technology 200.; Proc.* Of the Topical session: Experimental and theoretical investigations on boron dilution transients in PWRs. pp. 5-22. 2003.

Prasser, H.-M., Böttger, A., Zschau, J. A new electrode-mesh tomograph for gas liquid flows. *Flow Measurement and Instrumentation 9*, 111 ff., 1998.

Schaffrath A., Fischer, K.-C., Hahm, T., Wussow, S. Validation of the CFD Code Fluent by Post Test Calculation of the ROCOM Experiment T6655_21. *The 11th International Topical Meeting on Nuclear Reactor Thermal-Hydraulics (NURETH-11),* Popes' Palace Conference Center, Avignon, France. Paper: 141. 2005.